



Filler geometry and interface resistance of carbon nanofibres: Key parameters in thermally conductive polymer composites

Kati Gharagozloo-Hubmann, André Boden, Gregor J. F. Czempiel, Izabela Firkowska, and Stephanie Reich

Citation: [Applied Physics Letters](#) **102**, 213103 (2013); doi: 10.1063/1.4807420

View online: <http://dx.doi.org/10.1063/1.4807420>

View Table of Contents: <http://scitation.aip.org/content/aip/journal/apl/102/21?ver=pdfcov>

Published by the [AIP Publishing](#)

Articles you may be interested in

[Thermal conductivity of high performance carbon nanotube yarn-like fibers](#)

J. Appl. Phys. **115**, 174306 (2014); 10.1063/1.4874737

[Enhanced thermal conductivity of carbon fiber/phenolic resin composites by the introduction of carbon nanotubes](#)

Appl. Phys. Lett. **90**, 093125 (2007); 10.1063/1.2710778

[Thermal conductivity and interfacial resistance in single-wall carbon nanotube epoxy composites](#)

Appl. Phys. Lett. **87**, 161909 (2005); 10.1063/1.2103398

[Effects of chemical modifications on the thermal conductivity of carbon nanotube composites](#)

Appl. Phys. Lett. **86**, 123106 (2005); 10.1063/1.1887839

[Interface effect on thermal conductivity of carbon nanotube composites](#)

Appl. Phys. Lett. **85**, 3549 (2004); 10.1063/1.1808874

The advertisement features a dark blue background with a photograph of the Model PS-100 cryogenic probe station. The station is a complex piece of equipment with various mechanical components, including a probe head and a base. The text is arranged as follows: on the left, 'Model PS-100' is written in a large, bold, white font, with 'Tabletop Cryogenic Probe Station' in a smaller white font below it. On the right, the 'Lake Shore CRYOTRONICS' logo is displayed, consisting of a stylized blue and white square icon followed by the brand name in white. Below the logo, the tagline 'An affordable solution for a wide range of research' is written in a white, italicized font.

Filler geometry and interface resistance of carbon nanofibres: Key parameters in thermally conductive polymer composites

Kati Gharagozloo-Hubmann,^{a),b)} André Boden, Gregor J. F. Czempiel, Izabela Firkowska,^{b),c)} and Stephanie Reich

Department of Physics, Freie Universität Berlin, Arnimallee 14, 14195 Berlin, Germany

(Received 24 January 2013; accepted 24 April 2013; published online 28 May 2013)

The thermal conductivity of polymer composites is measured for several tubular carbon nanofillers (nanotubes, fibres, and whiskers). The highest enhancement in the thermal conductivity is observed for functionalized multiwalled carbon nanotubes (90% enhancement for 1 vol. %) and Pyrograf carbon fibres (80%). We model the experimental data using an effective thermal medium theory and determine the thermal interface resistance (R_K) at the filler-matrix interface. Our results show that the geometry of the nanofibres and the interface resistance are two key factors in engineering heat transport in a composite. © 2013 AIP Publishing LLC. [<http://dx.doi.org/10.1063/1.4807420>]

Carbon is the element with the largest structural diversity. It has various modifications, including the well-known polymorphs like graphite and diamond, and the nanosized fullerene and carbon nanotube. With the exception of diamond with sp^3 hybridized three-dimensional carbon network, the carbon modifications exhibit planar or curved structures with sp^2 -bonded carbons. Due to the sp^2 hybridization, carbon is chemically inert and mechanically stable. At the molecular level, heat transfer through non-metallic structures is dominated by crystal lattice vibrations, and most allotropes of carbon show high thermal conductivity. The microscopic size of carbon nanotubes makes the experimental determination of the thermal conductivity of an individual nanotube challenging. Nevertheless, the measured value of thermal conductivity of an individual carbon nanotube reached up to 3000 W/mK at room temperature.^{1,2} Free-standing graphene has a conductivity of 5300 W/mK.³ The thermal conductivity of bulk samples of carbon nanotubes, however, is much lower (on the order of few 10 W/mK) than observed in individual tubes.⁴

To benefit from the exceptional thermal properties of carbon nanotubes in technical applications, they are embedded into a bulk matrix forming a nanocomposite material. The properties of such composites are predicted by various models of composites systems.⁵⁻⁷ Incorporation of carbon nanotubes into organic fluids and polymers improves the matrix thermal conductivity by a factor of two to three,⁸ which is much lower than expected from a mixture of the two materials. This leads to the question which key parameters are the best for superior thermal performance of the nanocomposites. Existing studies concentrated on individual parameters but did not evaluate the interplay of filler conductivity, interface resistance, and geometry.⁹⁻¹¹

In this paper, we investigate the influence of carbon nanomaterials with varying thermal conductivity and geometrical structure (length, diameter, aspect ratio, and shape)

on the effective thermal properties of polymer composites. Besides carbon filler surface functionalization, the proper choice of filler geometry is essential to significantly improve the heat conduction properties of polymers. The experimental data are complemented by effective medium theory that provides insight into the thermal interface resistance between carbon fibres and a host matrix.

Different types of tube-like carbon materials were investigated: multiwalled carbon nanotubes (MWCNTs, Fibermax), vapour-graphitized carbon fibre (VGCF, Showa Denko Carbon, Inc.), and vapour-grown carbon nanofibres (Pyrograf, Applied Sciences, Inc.). The oxidative functionalization of MWCNTs (MWCNT-COOH) was accomplished with a mixture of nitric acid 65% and sulphuric acid 96% (1:3). As polymer matrix we used a homogeneous melt from poly(ethylene glycol) 1000 (Carl Roth GmbH, Germany) and poly(ethylene glycol)-block-poly(propylene glycol)-block-poly(ethylene glycol) (Sigma-Aldrich, Germany) (1:2.6). In this matrix the carbon fillers were dispersed using an ultrasound probe (Bandelin Sonopuls HD2070).

The homogenous mixture of polymer dispersion was casted into custom-made disk-shaped rubber mold for curing at RT. The thermal conductivity of the obtained polymer composites was measured with Hot Disk Transient Plane Source TPS 2500 apparatus (Hot Disk AB). In a standard measurement the sensor, which is composed of a double spiral nickel wire ($\varnothing \sim 4.002$ mm), was sandwiched between two pieces of the sample. The sensor served both as heat source and as temperature detector. From the recorded temperature curve over time, the thermal conductivity was obtained. Investigations were performed at room temperature.

Figure 1 shows scanning (SEM) and transmission electron microscopy (TEM) images of the tube-like carbon materials used in this work. The diameters, length, and aspect ratio of the nanocarbons were determined from the images. They are summarized in Table I together with other key physical properties. Multiwalled carbon nanotubes (Fig. 1(a)) and Pyrograf fibres (Fig. 1(b)) have hollow cylindrical structures that are depicted as schematic drawings in the bottom panels of Fig. 1. Multiwalled nanotubes have the

^{a)}Electronic mail: k.hubmann@fu-berlin.de.

^{b)}K. Gharagozloo-Hubmann and I. Firkowska contributed equally to this work.

^{c)}Electronic mail: ifirkowska@googlemail.com.

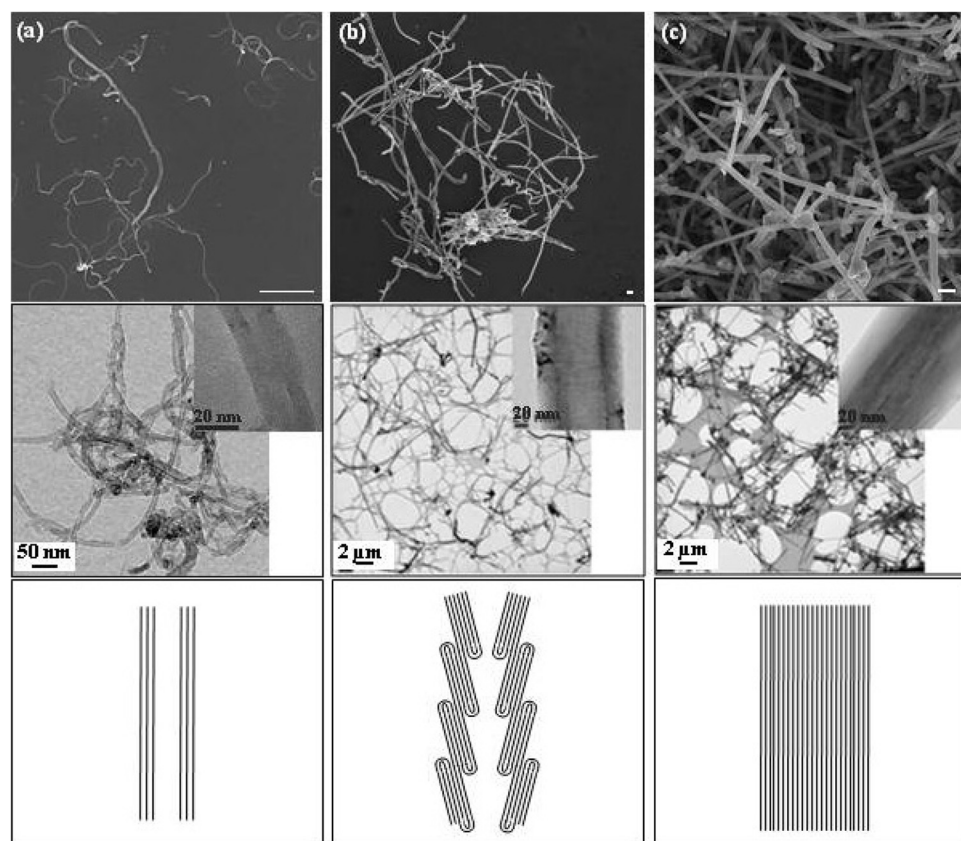


FIG. 1. SEM (upper row; scale bar 500 nm), TEM (middle row) micrographs, and schematic representation images (bottom) of MWCNTs (a), Pyrograf fibres (b), and carbon wire-VGCF (c).

highest thermal conductivity and the smallest dimensions (diameter, length) of the structures studied here. The Pyrograf fibres are almost six times longer than the MWCNTs, but their aspect ratios are similar to the tubes. The fibres are less entangled than the tubes since the larger fibre diameter and increased number of walls yield a greater rigidity (form stability). Finally, the Pyrograf fibres have a tilted wall pattern and much lower thermal conductivity than carbon nanotubes (Table I). In contrast to the hollow nanostructures in Figs. 1(a) and 1(b) the VGCF wires are compact and completely filled. The wires appear rigid and unbent (Fig. 1(c)). The VGCF wires have the lowest aspect ratio and thermal conductivity, but the largest diameter.

Figure 2 presents the measured thermal conductivity λ for carbon-polymer composites as a function of filler loading. The uncertainty in λ is estimated to be on the order of 10^{-2} W/mK based on analysing a batch of samples with identical filler volume fraction. Under the same conditions the thermal conductivity of pristine polymer was measured resulting in $\lambda = 0.18$ W/mK. Pristine MWCNTs yield the weakest thermal conductivity enhancement despite their superior thermal conductivity (see Table II). Particularly noticeable is the four-fold improvement in the slope of the

thermal conductivity with filler content after the oxidative functionalization of the MWCNTs. As for Pyrograf, the thermal conductivity per volume fraction is comparable to functionalized MWCNTs. The increase of the polymer thermal conductivity by VGCF is two times than for pristine MWCNT (Table II). Thereby, the VGCF reaches only 47% of improvement effect of Pyrograf or oxidized MWCNT.

When comparing the composite materials with untreated carbon fillers, it is interesting to note that MWCNTs having the highest conductivity gave the weakest improvement.^{9–11} The composite thermal conductivity depends strongly on secondary aspects such as filler size, geometry, and interface quality.^{15,16}

We use the effective medium approximation (EMA)^{17,18} to model the composite thermal properties. Our model takes into account the thermal properties of the components and their size and shape as well as the thermal resistance at the filler/matrix interface. Assuming randomly oriented, non-interacting fillers, the ratio between the thermal conductivity of the composite and the pure polymer matrix is given by¹⁸

$$\frac{\lambda_e}{\lambda_m} = \frac{3 + f(\beta_x + \beta_z)}{3 - f\beta_x}, \quad (1)$$

TABLE I. Characteristic dimensions and physical properties of carbon nanofillers.

	Density (g/cm ³)	Diameter-outer (nm)	Diameter-inner (nm)	Number of walls	Length (μ m)	Aspect ratio	λ (W/mK)
MWCNT	1.83	20	8	16	2	100	3000 (Refs. 1 and 2)
VGCF	2.23 ^a	150	0	112	8	53	1200 (Ref. 13)
Pyrograf	1.95	115	51	70	12	104	1950 (Ref. 14)

^aBased on the wire-like morphology of VGCF fibres, we assumed that their density is similar to graphite.¹²

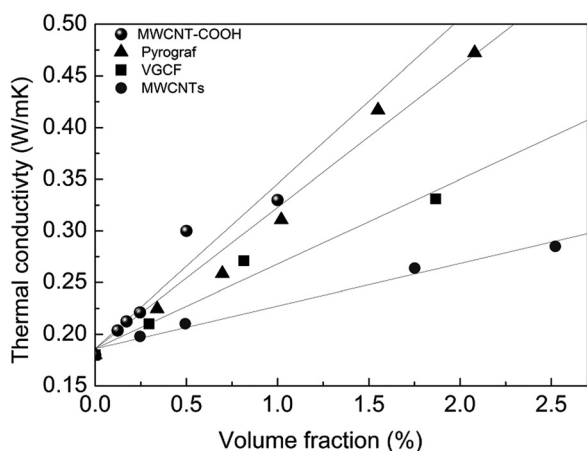


FIG. 2. Thermal conductivity of the fibre-polymer composites as function of the filler volume loading fraction.

with

$$\beta_x = \frac{2(\lambda_{11}^F + \lambda_m)}{\lambda_{11}^F + \lambda_m}, \quad \beta_z = \frac{\lambda_{33}^F}{\lambda_m} - 1, \quad (2)$$

where λ_e , λ_F , and λ_m are the thermal conductivities of the composite, carbon fibres, and matrix, respectively; f is the filler volume fraction; and λ_{11} and λ_{33} are equivalent thermal conductivities along the transverse and longitudinal axes of a composite unit cell and can be expressed as

$$\lambda_{11}^F = \frac{\lambda_F}{1 + (2a_K/d)(\lambda_F/\lambda_m)}, \quad \lambda_{33}^F = \frac{\lambda_F}{1 + (2a_K/L)(\lambda_F/\lambda_m)}, \quad (3)$$

where d is the diameter and L the length of the fillers. The so-called Kapitza radius is defined as

$$a_K = R_K \lambda_m. \quad (4)$$

The thermal conductivities λ for matrix (0.18 W/mK) and carbon nanofillers were taken from the literature. They are listed in Table I together with the average diameters and lengths of the fillers. The thermal interface resistance in carbon fibre composites was obtained from a fit to the experimental data with Eqs. (1) and (2). Depending on filler type and treatment R_K varies between $2 \times 10^{-8} \text{ m}^2 \text{ K/W}$ and $15 \times 10^{-8} \text{ m}^2 \text{ K/W}$ (see Table II).

The interface resistance of as-received carbon nanotubes ($7.3 \times 10^{-8} \text{ m}^2 \text{ K/W}$), Fig. 3, is in good agreement with the value obtained from picoseconds transient absorption

TABLE II. Thermal conductivity enhancement given by a slope fitted to the data from Fig. 2 and the calculated Kapitza resistance for our nanofibre composites.

	Slope(W/mK)	$R_K(\text{m}^2 \text{ K/W})$
MWCNT	4×10^{-2}	7.3×10^{-8}
MWNT-COOH	17×10^{-2}	2×10^{-8}
VGCF	8×10^{-2}	15×10^{-8}
Pyrograf	17×10^{-2}	12×10^{-8}

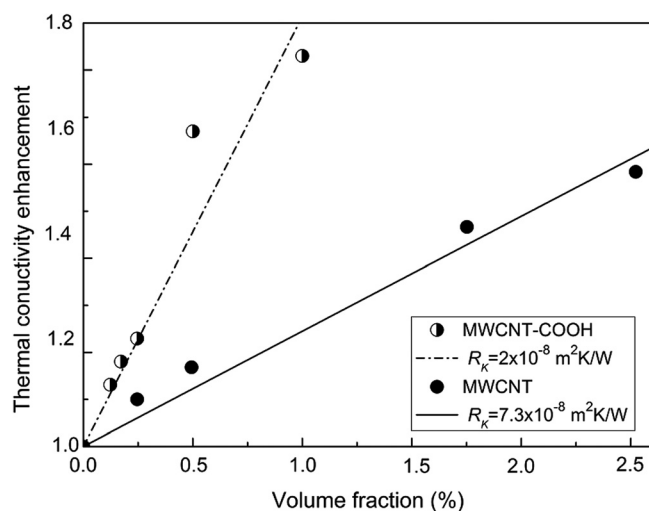


FIG. 3. Measured thermal conductivity enhancement of multiwalled nanotube-polymer composites with fitted theoretical curves for extraction of the Kapitza resistance. Note the impact of chemical surface modification on R_K value.

measurements of carbon nanotubes (CNTs) suspended in surfactant micelles in water ($8.3 \times 10^{-8} \text{ m}^2 \text{ K/W}$).¹⁹ This implies that the thermal properties of the composites are determined by the properties of the matrix and the nanofillers. We can rule out, e.g., an insufficient dispersion as a limiting factor for the rather poor thermal improvement upon nanotube loading. The Kapitza resistance of the chemically functionalized carbon nanotubes is four times lower than that of untreated nanotubes (Fig. 3) yielding a much higher thermal conductivity enhancement. The difference in Kapitza resistance results from the carboxyl groups attached to the functionalized CNTs. They improve the coupling of the nanoinclusion in the matrix molecules and facilitate the heat transfer to the surrounding polymer material.

As the surface modification gives a clear contribution to lower R_K it was interesting to study whether the morphology of non-chemically treated fibres is an alternative for improving the thermal resistance at the fibre-matrix interface. Looking at the unique structure of the Pyrograf fibres one expects that the exposed edge planes along the entire surface of the fibres might provide a better thermal contact with the polymer matrix. However, Kapitza resistance of the fibres is an order of magnitude above the resistance for functionalized nanotubes. There is no difference in R_K between the Pyrograf and the VGCF (Table II), indicating modest impact of the surface morphology.

Despite their low intrinsic thermal conductivity (Table I) and the high Kapitza resistance, Pyrograf fibres yield the highest thermal conductivity among our composites with untreated carbon fillers. This phenomenon can be understood when looking at the thermal conductivity enhancement as a function of the fibre length. As shown in Fig. 4, for the same volume fraction long Pyrograf fibres $L = 12 \mu\text{m}$ yield in 30% larger conductivity enhancement than the short carbon nanotubes ($L = 2 \mu\text{m}$). Considering the thermal conductivity of Pyrograf fibres as high as 3000 W/mK, i.e., equivalent to MWCNTs, only minor changes in the conductivity enhancement are visible. Significant drop in λ enhancement would be observed for fibres with conductivity of 500 W/mK

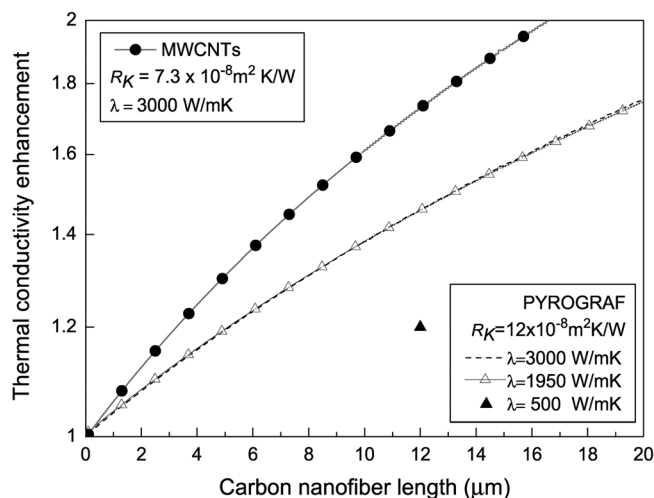


FIG. 4. Effect of fibre length on thermal conductivity enhancement predicted by the model Eq. (1) for 1 vol.%. Note that reducing intrinsic properties of Pyrograf fibres to 500 W/mK leads to the conductivity enhancement comparable to short MWCNTs.

(separate point in Fig. 4). However, by keeping the length of 12 μm , the obtained enhancement would be still as high as for the short and highly conductive MWCNTs. This clearly shows that the filler geometry is the second key parameter in optimizing thermal properties of polymer composites.

In conclusions, we examined the effects of the intrinsic thermal conductivity, geometry, and Kapitza resistance of tubular carbon fillers on the thermal performance of polymer composites. The interface thermal resistance and the length of the fibres dominate the effective thermal conductivity of composites, rather than a high intrinsic thermal conductivity of the fibres. The results show that using long carbon nanofibre with reduced thermal-interface resistance by surface

functionalization is the most efficient way to engineer composite material with good thermal conductivity.

The authors thank the Federal Ministry of Education and Research, BMBF (Grant no. CNTherm 482102-01/02 and VIP 0420482104) and BMWi (Grant No. EXIST 0420482103) for financial support and Ms. G. Weinberg from FHI for SEM investigations and S. Selve (Technical University Berlin) for TEM investigations.

- ¹J. Hone, M. Whitney, and A. Zettl, *Synth. Met.* **103**, 2498 (1999).
- ²P. Kim, L. Shi, A. Majumdar, and P. L. McEuen, *Phys. Rev. Lett.* **87**, 215502 (2001).
- ³A. A. Balandin, S. Ghosh, W. Bao, I. Calizo, D. Teweldebrhan, F. Miao, and C. N. Lau, *Nano Lett.* **8**, 902 (2008).
- ⁴P. Gonneta, Z. Lianga, E. S. Choib, R. S. Kadambalaa, C. Zhanga, J. S. Brooks, B. Wang, and L. Kramer, *Curr. Appl. Phys.* **6**, 119 (2006).
- ⁵B.-X. Wang, L.-P. Zhou, and X.-F. Peng, *Int. J. Heat Mass Transfer* **46**, 2665 (2003).
- ⁶I. L. Skryabin, A. V. Radchik, P. Moses, and G. B. Smith, *Appl. Phys. Lett.* **70**, 2221 (1997).
- ⁷Q. Z. Xue, *Nanotechnology* **17**, 1655 (2006).
- ⁸F. Wu, X. He, Y. Zeng, and H.-M. Cheng, *Appl. Phys. A* **85**, 25 (2006).
- ⁹S. Shenogin, A. Bodapati, L. Xue, R. Ozisik, and P. Keblinski, *Appl. Phys. Lett.* **85**, 2229 (2004).
- ¹⁰Z. Han and A. Fina, *Prog. Polym. Sci.* **36**, 914 (2011).
- ¹¹S. Y. Pak, H. M. Kim, S. Y. Kim, and J. R. Youn, *Carbon* **50**, 4830 (2012).
- ¹²C. Laurent, E. Flahaut, and A. Peigney, *Carbon* **48**, 2994 (2010).
- ¹³Y.-M. Chen and J.-M. Ting, *Carbon* **40**, 359 (2002).
- ¹⁴J. J. George and A. K. Bhowmick, *Nanoscale Res. Lett.* **4**, 655 (2009).
- ¹⁵I. Firkowska, A. Boden, A.-M. Vogt, and S. Reich, *J. Mater. Chem.* **21**, 17541 (2011).
- ¹⁶A. A. Balandin, *Nat. Mater.* **10**, 569 (2011).
- ¹⁷C.-W. Nan, Z. Shi, and Y. Lin, *Chem. Phys. Lett.* **375**, 666 (2003).
- ¹⁸C.-W. Nan, G. Liu, Y. Lin, and M. Li, *Appl. Phys. Lett.* **85**, 3549 (2004).
- ¹⁹S. T. Huxtable, D. G. Cahill, S. Shenogin, L. Xue, R. Ozisik, P. Barone, M. Usrey, M. S. Strano, G. Siddons, M. Shim, and P. Keblinski, *Nat. Mater.* **2**, 731 (2003).